Civil Engineering Infrastructures Journal, 48(2): 217-234, December 2015
ISSN: 2322-2093

An Adaptive Physics-Based Method for the Solution of One-Dimensional Wave Motion Problems

Shafiei, M.[1] and Khaji, N.[2*]

[1] Ph.D., Faculty of Civil and Environmental Engineering, Tarbiat Modares University, Tehran, Iran.

[2] Professor, Faculty of Civil and Environmental Engineering, Tarbiat Modares University, Tehran, Iran.

Received: 20 Jan. 2014 Revised: 17 Jan. 2015 Accepted: 10 Mar. 2015

Abstract: In this paper, an adaptive physics-based method is developed for solving wave motion problems in one dimension (i.e., wave propagation in strings, rods and beams). The solution of the problem includes two main parts. In the first part, after discretization of the domain, a physics-based method is developed considering the conservation of mass and the balance of momentum. In the second part, adaptive points are determined using the wavelet theory. This part is done employing the Deslauries-Dubuc (D-D) wavelets. By solving the problem in the first step, the domain of the problem is discretized by the same cells taking into consideration the load and characteristics of the structure. After the first trial solution, the D-D interpolation shows the lack and redundancy of points in the domain. These points will be added or eliminated for the next solution. This process may be repeated for obtaining an adaptive mesh for each step. Also, the smoothing spline fit is used to eliminate the noisy portion of the solution. Finally, the results of the proposed method are compared with the results available in the literature. The comparison shows excellent agreement between the obtained results and those already reported.

Keywords: Adaptive solution, Deslauries-Dubuc wavelets, Multi-resolution analysis, Physics-based solution, Smoothing splines.

INTRODUCTION

Discrete computation methods such as the cellular automaton (CA) method and the lattice gas automaton method have been already introduced to analyze numerous problems in various fields of engineering. In this paper, the CA method is used for the solution of wave motion problem in one dimension. The CA method was first developed by von Neumann (1966) in Los Alamos National Lab. Different types of the CA (e.g., deterministic or probabilistic, and/or continuous or totalistic) are currently being presented and implemented for various kinds of science and engineering problems. As the CA systems are intrinsically dynamic, this method may be implemented to tackle problems which involve dynamic behavior. In the CA method, the analysis domain is divided into similar finite parts called "cells". The state of each cell is updated according to local rules at every discrete time step. The state of a cell at a given time step depends only on its previous state and those of its neighbor cells. The states of all cells are updated synchronously. As a result of such computational characteristics, solution can be performed for only the desired portion of the entire domain. In the last three

* Corresponding author Email: nkhaji@modares.ac.ir

decades, the CA method has been used to model different problems, among which some remarkable works are cited here. Frisch et al. (1987) implemented the CA to model two- and three-dimensional simulations of lattice gas hydrodynamics problems. Using a two-dimensional CA, Rothman (1987) simulated the propagation of seismic P-waves in a homogeneous medium. Chopard and Droz (1988) employed the approach to analyze non-equilibrium phase transitions in surface reaction models, based on static and dynamic properties of the undertaken domain. Using the CA method, Chopard et al. (1989) solved the non-equilibrium diffusion and gradient percolation problems. Afterwards, Chopard (1990) used this method to model large scale moving objects such as propagation of sound waves. Schreckenburg et al. (1995) and Chopard et al. (1996) developed the CA method to model traffic flow. In 2002, a serious evolution occurred in CA's employment in solving various problems, after the publication of Wolfram (2002) book. Kawamura et al. (2005, 2006) used the CA method to model wave propagation in a nonlinear vibrating string using differential equations and reflection rule. The combination of reflection rule and the CA method was implemented by Kwon and Hosoglu (2008) for modeling SH-wave propagation in two dimensions. Leamy (2008) derived equations of wave propagation in two dimensional problems (lamb wave) using the bottom-up nature of the CA method for rectangular cells. Hopman and Leamy (2011) introduced triangular automata for two dimensional elastodynamic problems.

The CA's paradigm may be distinguished from other numerical methods' paradigm in different aspects. The afore-mentioned researches emphasized on the specific property of the method. Derivation of neighborhood rules is the most crucial issue in problems to be solved by the CA. Some researchers derived these rules by considering relevant differential equations, whereas others tried to make these rules by considering the laws of physics (e.g., mass conservation and momentum balance rules in elastic wave propagation problems). Common numerical methods (e.g., Finite Element, Finite Difference and Boundary Element methods) use corresponding differential equations of the problem to derive the formulation of the problem to be solved. On the other hand, some researchers used the CA for similar problems in such a way that neighborhood rules were derived from related concepts in physics. In fact, a principally distinguishing aspect of the CA modeling is its application for the solution of physics-based formulated problems. Briefly, in the CA method, each part (or, cell) of the solution domain shows a relatively independent role. The behavior of each cell depends on its neighbors, whereas in other mentioned numerical methods, differential equation acts in the whole domain. This feature distinguishes the CA from other numerical methods, and leads to remarkable computational advantages. Despite these advantages, the CA has some shortcomings. In definition, the CA divides the solution domain into a number of cells with their own dimensions and properties. An accurate solution of a problem with low computational cost may be obtained, when discretization of the solution domain and/or order of the solution are appropriate to the complexity level of the solution. For this purpose, various methods were employed in recent years, among which the Deslauries-Dubuc (D-D) (1989) interpolating wavelets are very popular.

In this study, these two concepts (i.e., physics-based formulation and the D-D interpolating wavelets) are used to solve the wave motion problem in one dimension (that is, string, rod, and beam problems) in an adaptive form. In the next section, the D-D interpolating wavelets are discussed, and then the formulation of

physics-based solution is presented afterwards.

METHODOLOGY

The D-D Interpolating Wavelets

Adaptive wavelet grid-based methods were successfully applied in elliptic, parabolic and hyperbolic partial differential equations (PDEs) by Cruze et al. (2001), Liu et al. (2000), Jameson (1998), Vasilyev and Paolucci (1996) and Holmström (1999). Special characteristics of the wavelet concept such as complete multi-resolution property, fast algorithms and data compression ability, posed this method as a fast versatile tool for various purposes. In multi-resolution analyses, each wavelet coefficient may be linked to a given point of the underlying grid. The solution of the problem begins through the same cells. In this regard, centroid to each cell is a solution point, as well as a sample for multi-resolution analysis. Depending on the gradient of the solution, cells should be regenerated in finer or coarser forms in some regions. In order to achieve a good resolution in all parts of the solution domain, this process has to be repeated.

Assume *j* is a scale level for the solution of the first step. At the coarser level (i.e., *j*-1), the D-D interpolating scheme can predict the eliminated values. The difference of eliminated value and predicted value in each solution point shows whether each point is needed at level *j*, or not. In each point, this comparison is independent of other points of the solution domain. In some parts of the solution domain, on the other hand, the initial resolution may not be sufficient. In these parts, new solution points should be added in the middle point of current solution points (i.e., level *j*+1). This process may be continued until the solution values and predicted values (from a coarser level) reach an acceptable difference. More details of the approach are illustrated in the next sections.

The CA Formulation for Vibration of String

In the first step, the solution domain is divided into equal parts (or, cells) as shown schematically in Figure 1, in which each cell has two neighbors. For example, the *i*th cell is in the neighborhood with cells *i*+1 and *i*-1.

As shown in Figure 1, black points separate the cells from each other, while cross sign (i.e., mid-points of the cells) are assumed as solution points. As discussed earlier, this mesh would be used only in the first step of the solution. In general, the presented solution may be used for both regular and irregular meshes.

The solution of the problem using the CA method is mainly the derivation of local rules for all possible conditions. As previously discussed, in comparison with other numerical methods, the CA uses local rules to solve a problem. In the establishment of equations, the balance of forces is considered on a discrete cell, which results in global equations called "rules." Figure 2 assumes a cell of a vibrating string. In this figure, the *x*-axis is assumed to be in the string's direction when the string has no displacement. The *y*-axis is normal to the *x*-axis in the plane.

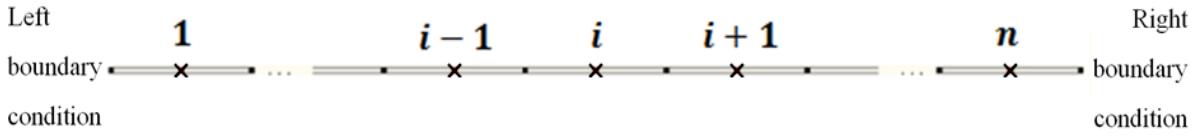

Fig. 1. The string problem, in which cells (separated by points), solution points (indicated by cross sign), and boundary conditions are drawn

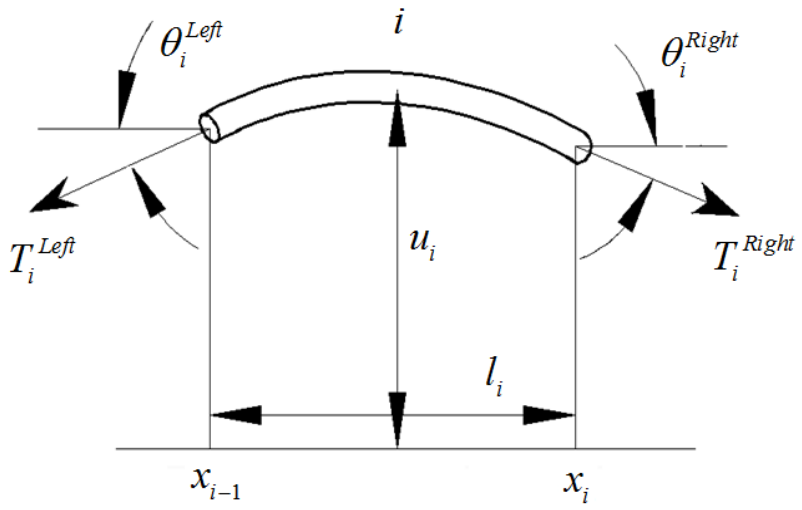

Fig. 2. A part of the string along with applied forces

As shown in Figure 2, the internal forces of the *i*th cell, in the *y*-direction, may be written as:

$$ {}_iF_y^{Left} = T_i^{Left} \sin\theta_i^{Left} \quad (1)$$

$$ {}_iF_y^{Right} = T_i^{Right} \sin\theta_i^{Right} \quad (2)$$

In the linear vibration of a string, both angles of θ^{Left} and θ^{Right}: are assumed to be small, and therefore $\cos\theta^{Left} = \cos\theta^{Right} = 1$. As a result, the net horizontal force is equal to zero and $\sin\theta^{Left} = \tan\theta^{Left}$, and $\sin\theta^{Right} = \tan\theta^{Right}$. Based on the values of neighbor cells, $\tan\theta^{Right}$ and $\tan\theta^{Left}$ would be available. Consequently, Eqs. (1) and (2) may be rewritten as:

$$ {}_iF_y^{Left} = T_i^{Left} \sin\theta_i^{Left} = 2T_i^{Left} \frac{u_i - u_{i-1}}{l_i + l_{i-1}} \quad (3)$$

$$ {}_iF_y^{Right} = T_i^{Right} \sin\theta_i^{Right} = 2T_i^{Right} \frac{u_{i+1} - u_i}{l_{i+1} + l_i} \quad (4)$$

whose parameters are introduced in Figure 2. The balance of momentum for the *i*th cell yields in the following equation:

$$ \overline{m}_i l_i a_i = F_{External} + ({}_iF_y^{Right} - {}_iF_y^{Left}) \quad (5)$$

where $F_{External}$ and a_i: are the external force and the acceleration of the *i*th cell, respectively. Moreover, $\overline{m}_i$: denotes the linear mass of the *i*th cell. Knowing the acceleration of the cell in each step and using first-order updates, the velocity (v) and displacement (u) of each cell are available as:

$$ v^{j+1} = \frac{1}{n\overline{m}_i}[F_{External} + ({}_iF_y^{Right} - {}_iF_y^{Left})] + v^j \quad (6)$$

$$ u^{j+1} = \frac{1}{n} v^{j+1} + u^j \quad (7)$$

where n: represents the number of steps per unit of time. Time step size can be varied to satisfy the Courant's condition (Courant, 1928). Superscripts j and j+1, denote the values of each variable in steps j and j+1, respectively.

Furthermore, in the next step, the boundary conditions (BCs) should be considered in the most left and the most right cells of the domain. In the present research, two known BCs of Dirichlet and Neumann were taken into account. Satisfying Dirichlet BC, displacement, and velocity of each cell were set equal to zero (or a known value) at the end of each step.

For Neumann BC on the other hand, an imaginary cell should be used in the neighborhood of the free cell. In this imaginary cell, force is known and displacement would be determined in such a way that the known force is satisfied. For a known force value in the left end of the string (Figure 1), one may write

$$F_y^{Left} = T_1^{Left} \sin\theta_1^{Left} = T_1^{Left} \frac{u_1 - u_{\text{Im}}}{l_1} \qquad (8)$$

where u_{Im}: indicates the displacement of the imaginary cell. The length of the imaginary cell is considered to be equal to u_1. Furthermore, the following equation may be easily written:

$$u_{\text{Im}} = u_1 - \frac{F_1^{Left} l_1}{T_1^{Left}} \qquad (9)$$

The above procedure may be followed for a vibrating rod in a similar manner in order to derive its vibration formulation using the CA.

The CA Formulation for Vibration in a Beam

The well-known Euler-Bernoulli beam theory was used for derivation of the formulation. In this theory, the effect of shear deformation and rotary inertia was neglected. For the case of Euler-Bernoulli beam of this research, the radius-r CA with r=2 was employed (Figure 3).

For the *i*th cell, the radius of curvature is given by:

$$\frac{1}{R_i} = \frac{\left(\frac{d^2y}{dx^2}\right)_i}{\left[1+\left(\frac{dy}{dx}\right)_i^2\right]^{3/2}} \qquad (10)$$

where y: is the vertical deflection and x: indicates the location of the *i*th cells. In addition, the first- and second-order derivatives of y are given by the following well-known finite difference equations for regular cells:

$$\left(\frac{dy}{dx}\right)_i = \frac{y_{i+1} - y_{i-1}}{2\Delta x_i}, \qquad (11)$$

$$\left(\frac{d^2y}{dx^2}\right)_i = \frac{y_{i-1} - 2y_i + y_{i+1}}{\Delta x_i^{\,2}}, \qquad (12)$$

where Δx_i: denotes the length of the *i*th cell. In accordance with basic assumptions of bending in beams (Timoshenko, 1953), the bending moment of each cell is written as:

$$M_i = -\frac{E_i I_i}{R_i} \qquad (13)$$

in which E_i: is the Young's modulus, and I_i: denotes the moment of inertia. Figure 4 depicts the applied shear forces and bending moments to the *i*th cell of the domain.

As shown in Figure 4, the equilibrium equation for the y-direction may be written as:

$$V_i^{Right} - V_i^{Left} - q(x_i,t)\Delta x_i = \overline{m}_i \Delta x_i a_i \qquad (14)$$

where $q(x,t)$: is the external distributed force, and a_i: denotes the acceleration of the cell. Moreover, V_i^{Right} and V_i^{Left}: are shear force on the right and left sides of the cell. These forces may be easily obtainable from the following relations:

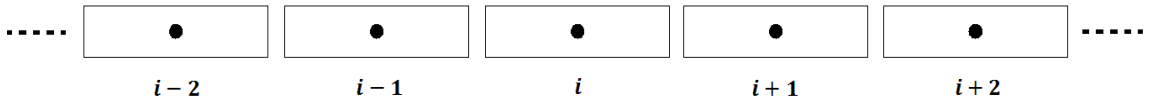

Fig. 3. The target cell (cell *i*) and the radius-r neighbors ($r = 2$)

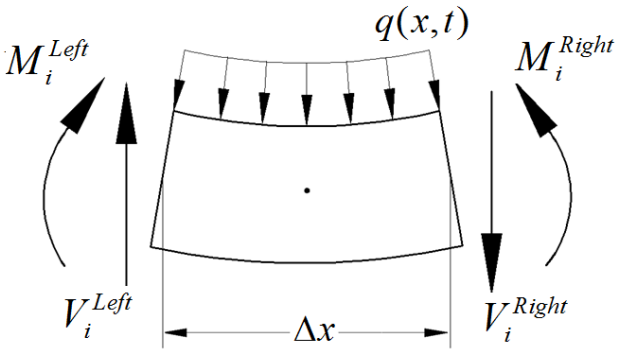

Fig. 4. Schematic view of a cell and applied internal and external loads

$$V_i^{Right} = \frac{M_{j+1} - M_j}{\Delta x_i} \quad (15)$$

$$V_i^{Left} = \frac{M_j - M_{j-1}}{\Delta x_i} \quad (16)$$

Furthermore, the right side and left side bending moment of the *i*th cell may be determined as:

$$M_i^{Right} = \frac{M_{j+1} + M_j}{2} \quad (17)$$

$$M_i^{Left} = \frac{M_j + M_{j-1}}{2} \quad (18)$$

Knowing the acceleration of the cell in each step and using first-order updates, velocity (*v*) and displacement (*y*) of each cell would be easily computed.

The BCs should be properly implemented in the next step of the problem solution. Obviously, various BCs are expected for the beam problem. Usually, among four existing parameters (i.e., bending moment, shear force, slope, and deflection of the beam), two parameters are known, while two others are unknown. These two known parameters may be combined in different manners. For the case of a known displacement for example, displacement of the boundary cell may be updated according to the known value (or, a set of known values in a time domain). For other BCs, depending on the type of the Neumann BCs, imaginary cells are added to the solution domain. In these imaginary cells, displacement may be determined in such a way that known parameters (i.e., bending moment, shear force, and/or slope of the beam) are satisfied.

Wavelet Concept and Adaptive Solution

Wavelets are usually introduced by defining scaling functions $\phi_{j,k}$, wavelets $\psi_{j,k}$, and the associated function spaces V_j (corresponding to $\phi_{j,k}$) and W_j (corresponding to $\psi_{j,k}$) (Mallat, 1999). Since an interpolating wavelet transform was used, it is possible to define the transform in terms of interpolation on dyadic grids, instead. First, we present the interpolating subdivision idea proposed by Deslauriers and Dubuc (1989). Assume that we have a set of dyadic grids on the real line as:

$$V_j = \left\{ x_{j,k} = 2^{-j}k \,\middle|\, x_{j,k} \in \mathbf{R},\, k \in \mathbf{Z},\; j \in \mathbf{Z} \right\} \quad (19)$$

where **R** and **Z**: denote the real and integer numbers, respectively. Figure 5 shows the locations of these points on the aforementioned grid.

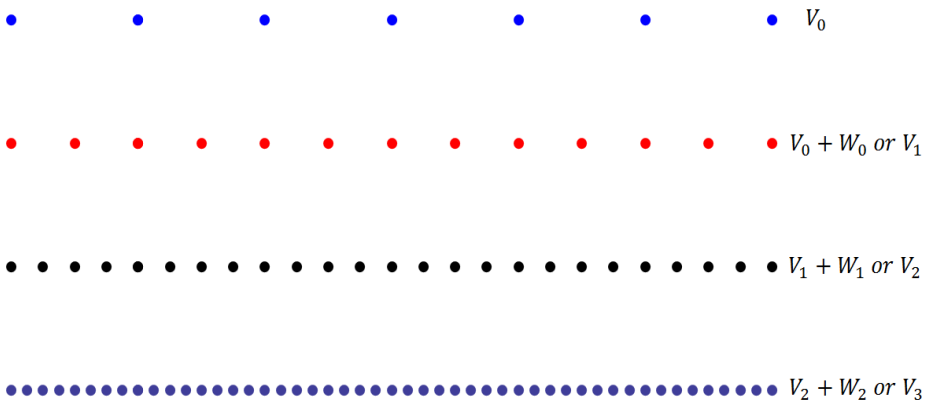

Fig. 5. The position of points in a dyadic grid

Let us assume that the given function values on V_j are denoted by $\{f_{j,k}\}$, where $f_{j,k} = f(x_{j,k})$: is a function defined on the grid points in V_j. Now, we would like to extend V_j to all points $f_{j+1,k}$ in V_{j+1}. The interpolating subdivision idea is a suitable algorithm to achieve this goal. For this purpose, the even-numbered grid points $x_{j+1,2k}$ are already in existence in V_j, therefore, the corresponding function values remain unchanged. The values at the odd-numbered grid points $x_{j+1,2k+1}$ were computed using polynomial interpolation from the values at the even-numbered grid points. The degree of this interpolating polynomial is $p-1$, as such we say that the interpolation is in order of p. The order is chosen to be even, in order to make the interpolation symmetric. As earlier discussed, the given function values on a coarse grid, and the interpolating subdivision idea generates function values on a finer grid. In the reverse direction, we could just throw away half of the grid points at each level, but we would lose some information. Instead, for odd-numbered grid points at each level, we may compute the difference between the known function value and the function value predicted by interpolation from the coarser grid. These differences in function values' wavelet coefficients are indicated by $d_{j,k}$. The computation of a wavelet coefficient is illustrated in Figure 6, for the case of a cubic curve ($p = 4$).

Repeating the mentioned procedure recursively, a new algorithm is established for computing the full wavelet representation from function values on a fine grid. The wavelet representation is illustrated in Figure 7.

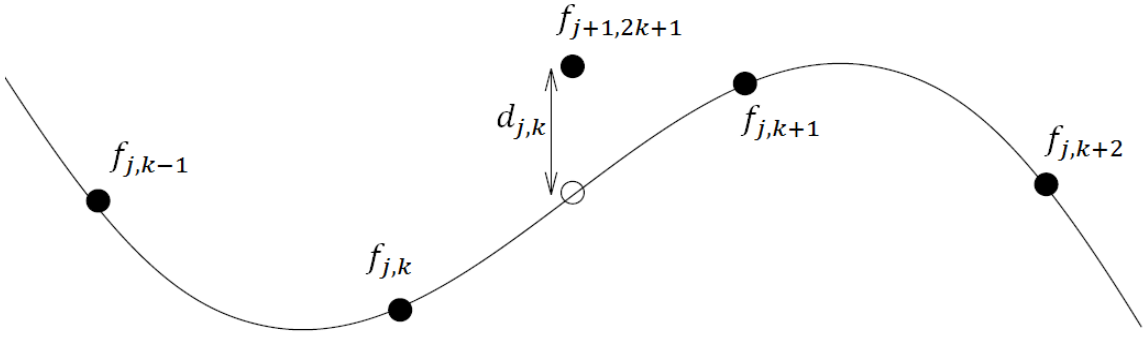

Fig. 6. Prediction of a known value from higher resolution using cubic curve, and determination of corresponding wavelet coefficient

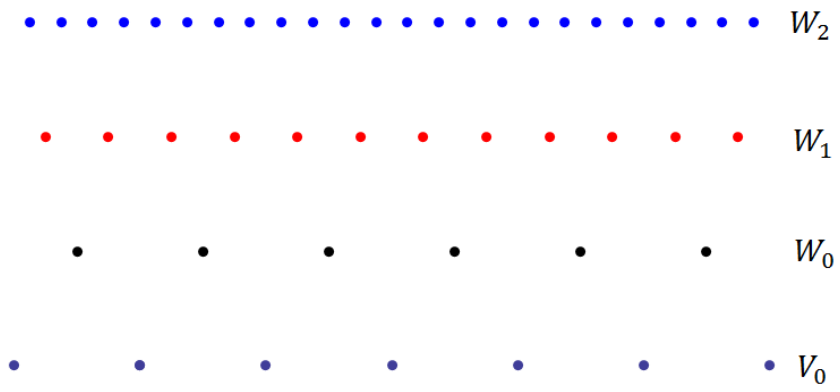

Fig. 7. Points in basis space (V_0) and the added points corresponding to added spaces (W_0 ,W_1 ,W_2) which are related to wavelets

After the above algebraic manipulations, sets of numbers in each level are available. Depending on the expected order of accuracy, some values of $d_{j,k}$ smaller than a specified threshold *e* may be eliminated. Considering these eliminations, a remarkable number of wavelet coefficients would be eliminated for the case of smooth function. The number of remaining coefficients mainly depends on the variation of the gradient in the original function. In conclusion, it should be noted that for the case of boundary grids, boundary wavelets introduced by Donoho (1992) were used in this work.

Smoothing of the Noisy Data

During the problem solving, various types of errors may occur. Depending on the type of problem, these errors may remain in the domain and create larger errors. When an adaptive solution is desired, these errors create erroneous adapted grid zones. Therefore, smoothing fit is adopted to eliminate the noisy portion of the solution. Smoothing function is constructed using the solution points (x_i, y_i), which are generally irregular. Let us assume that $f(x)$ is the smoothest function for the mentioned points. It is known that $f(x)$ may be obtained from minimizing the following functional:

$$F = \lambda \sum_{j=1}^{n} W_j \left| y_j - f(x_j) \right|^2 + \int_{-\infty}^{\infty} \left| f^{(m)}(x) \right|^2 dx \,,\ 0 \le \lambda < \infty \tag{20}$$

in which, λ and W_j: are Lagrangian parameter and weight factor at point *j*, respectively. In addition, *m*: denotes the derivative order. Odd degree splines ($\kappa = 2m-1$ with $2m-2$ continuous derivatives) have optimal solution for Eq. (20) (Reinsch, 1971). In this research, cubic spline $\kappa = 3$ was then employed (that is, $f \in C^2$). It is clear that the Lagrangian parameter (λ), sets the amount of smoothness. When λ approaches to infinity, Eq. (20) yields the usual interpolating spline, whereas $\lambda = 0$ corresponds to the least square straight line. For the mentioned interval, when λ decreases, the interpolating property vanishes, while the smoothing property increases. Accordingly, selection of the Lagrangian parameter is the most important part of the smoothing procedure. In this study, all sample points W_j are assumed to be unit. Considering the results of other studies, the Lagrangian parameter is assumed as $\lambda = 4$.

Based on the above explanations, the adaptive solution of the mentioned problems involves the following algorithm:

1. Select appropriate points for scale function.
2. Solve the problem for this level and then other existing ones at the finer level.
3. Apply the smoothing scheme for solution points and find the corrected solution.
4. Find the difference of the predicted values and the existing ones at the finer level.
5. Eliminate points for which $d_{j,k} < e$.
6. Refine the remaining mesh for regions where $d_{j,k} > e$ and solve the problem again. In this regard, the time step may change in accordance with Courant's condition.
7. Proceed to step 6, until there still exist any points where $d_{j,k} > e$.
8. Go to step 2 to solve the problem in the next time step.

NUMERICAL EXAMPLES

Forced Vibration of a Rod

The first example is related to longitudinal wave motion in a rod with zero initial conditions as shown in Figure 8. The rod's length is 10 m and the material properties of the rod are as follow: the Young's modulus $E = 210$ GPa, and the mass density $\rho = 7850\,\text{kg/m}^3$. The left end of the rod ($x = 0$) is fixed, while the right end ($x = 10\,m$) is subjected to a known stress time history as given:

$$\sigma(t) = \begin{cases} \sin(200\pi t^2); & 0 < t \le 0.2 \\ -\sin(200\pi (t-0.4)^2); & 0.2 < t \le 0.4 \\ 0\,; & t > 0.4 \end{cases} \quad (21)$$

where t: represents time (in milliseconds), and σ: represents the applied stress (in MPa). Smoothing scheme is employed for this problem with the mentioned Lagrangian parameter. In this case, the Lagrangian parameter was examined for the analytical solution with a random zero mean and variance noise. Random noise was eliminated from the solution, and the result is coincident with the original signal.

Fig. 8. The first example. A sample rod excited by an end stress field

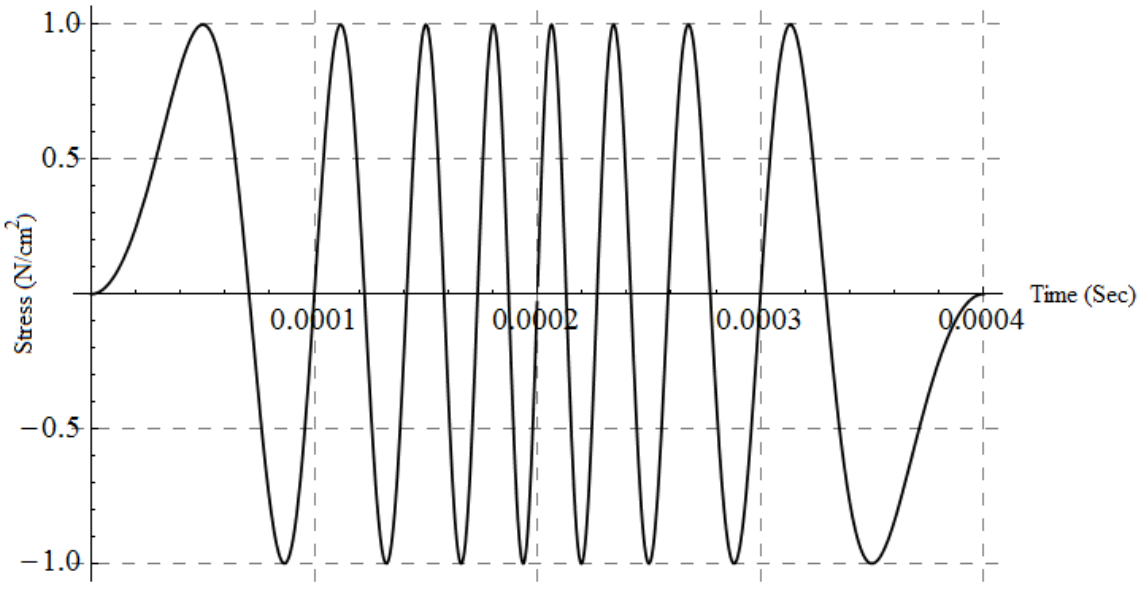

Fig. 9. The variation of applied external traction at the right end of the rod

The results of this study's method were compared with the analytical results obtained by Yang (2008). The comparisons show that the results of the two methods are identical and indistinguishable. Furthermore, the solution results of the study's method are given for three different time steps in Figure 10. Also, the horizontal displacement of the mid-point of the rod is shown in Figure 11.

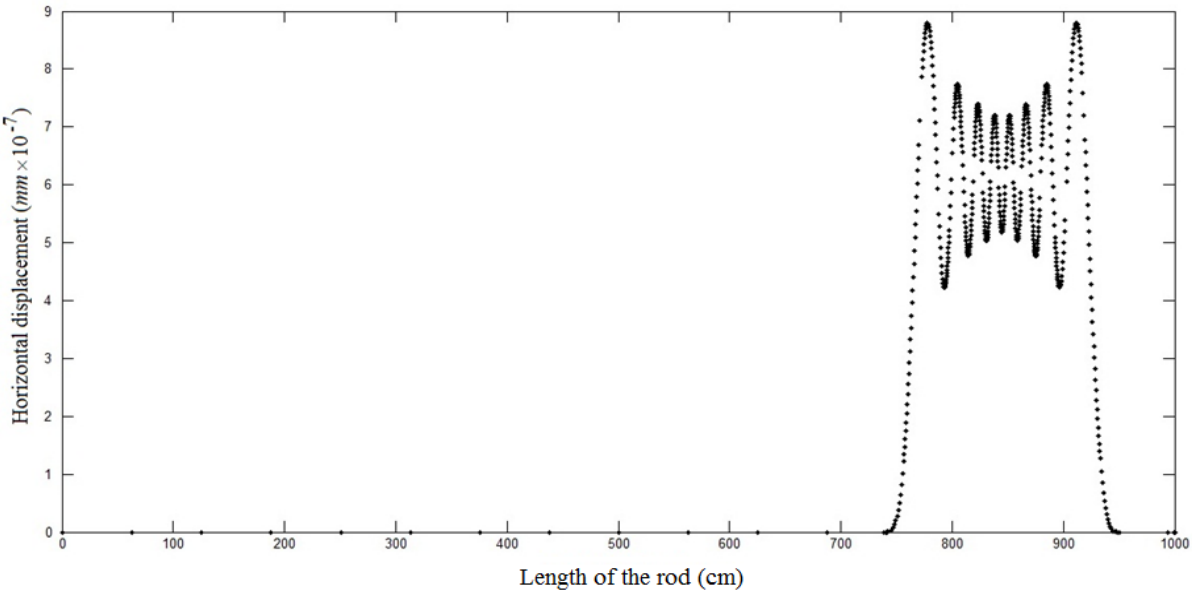

(a)

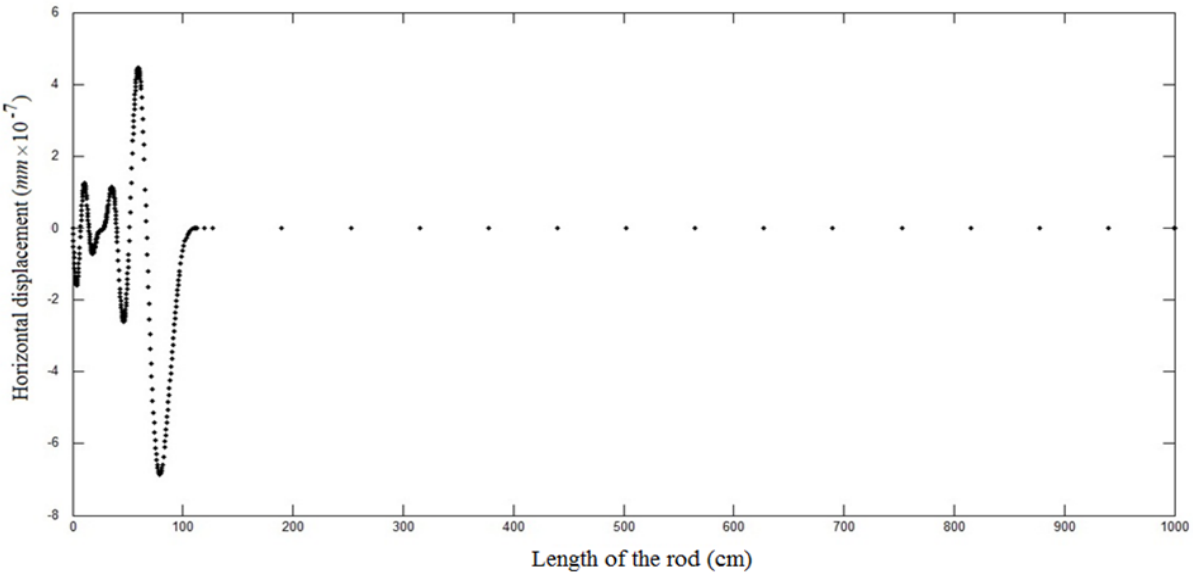

(b)

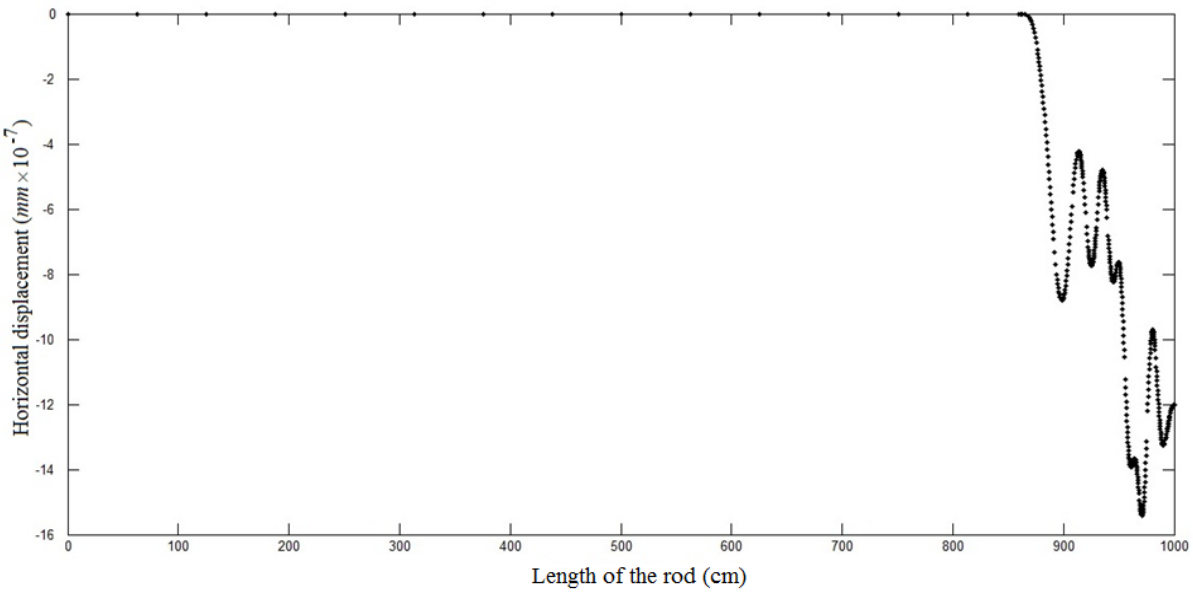

(c)

Fig. 10. Horizontal displacement of the rod at various time steps; (a) $t = 0.50$ ms, (b) $t = 2.15$ ms, (c) $t = 4.30$ ms

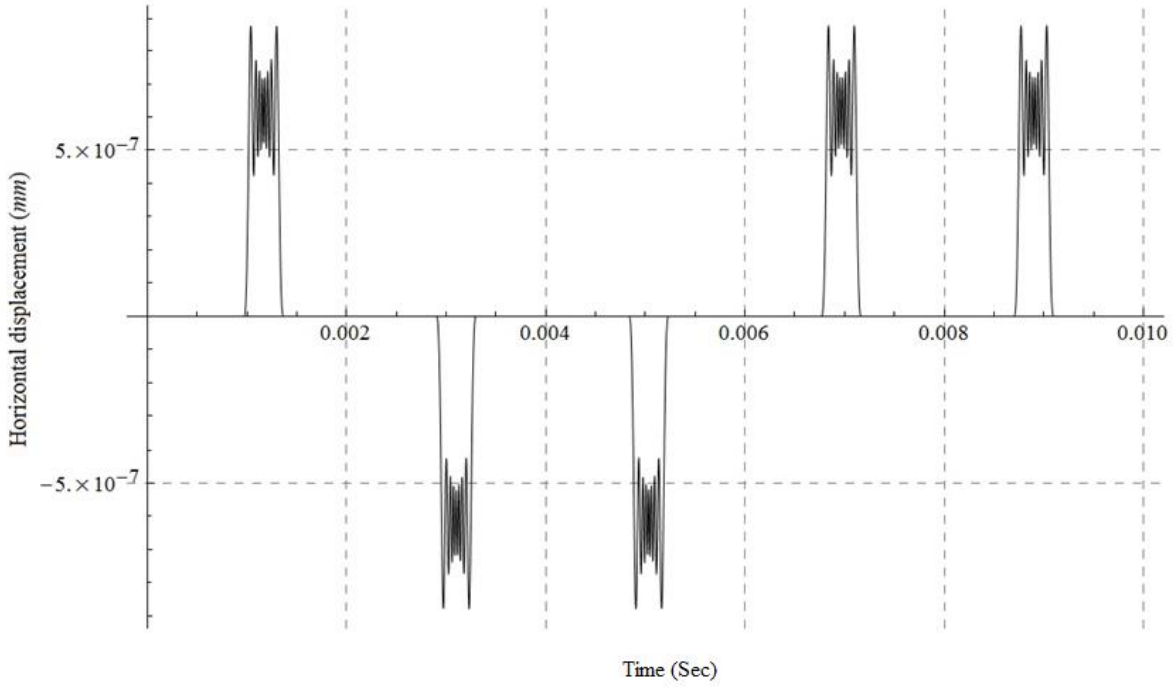

Fig. 11. Horizontal displacement of the rod ($x = 5$ m)

For this problem, the proposed algorithm was employed. It is remarkable that in a new time step in the time marching process, the solution begins with the adapted mesh of the previous time step. In the first step of this problem, the scale space is constructed by $2^4 + 1$ points. In addition, *j* and *e* are assumed as 9 and 1E–14, respectively.

Free Vibration of a String

The next example corresponds to wave propagation in a string with unit length and unit wave velocity. The initial velocity of the string is assumed to be zero in the

whole domain. The initial displacement of the string is represented by the following relation:

$$f(x)=\begin{cases}0.01(1+\cos(20\pi x)); & 0.45<x<0.55\\ 0 \quad ; & x>0.55 \text{ or } x<0.45\end{cases} \tag{22}$$

Results of this study's method were compared with the analytical solution achieved by d'Alambert's method (Yang, 2008). Again, the scale space was constructed by 2^4+1 points, which forms uniform cells. Although the D-D scheme can eliminate the redundant nodes in the scale space (corresponding to $j=-1$); however, this feature was not used in this example. Moreover, the D-D scheme may reconstruct an arbitrary function with minimum samples. Figure 12 shows that the function f in Eq. (22) has been reconstructed ($j=6$ and $e=1\text{E}-5$). Furthermore, the mentioned smoothing scheme is applied to this problem.

The results of the solution with this method are presented in three different time steps as shown in Figure 13. In this solution, the presented algorithm was used. It should be noted that in a new time step of the time marching process, the solution starts with the adapted mesh in the previous time step. For this example, *j* and *e* were selected as 6 and 1E–5, respectively.

Also, displacement of the string at point $x=0.25$ obtained by the study's method is compared with the analytical solution (Yang, 2008). When the results as plotted in Figure 14 were compared, the results of this study's method show excellent agreement with the analytical solution.

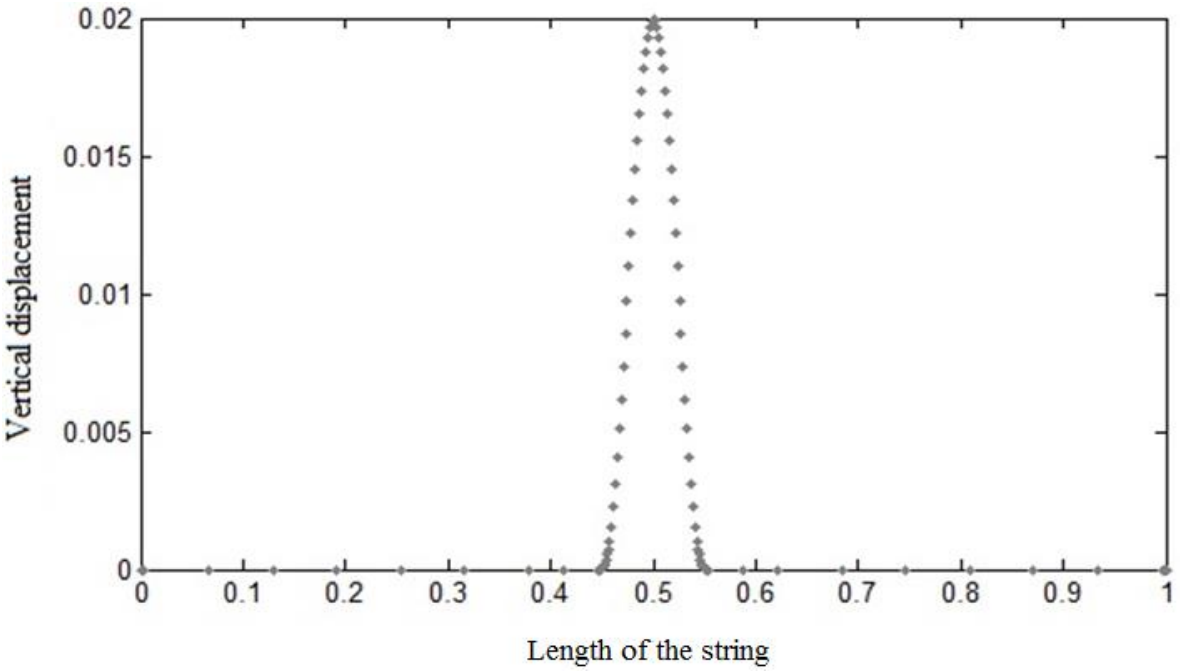

Fig. 12. Reconstruction of function *f* using the D-D scheme

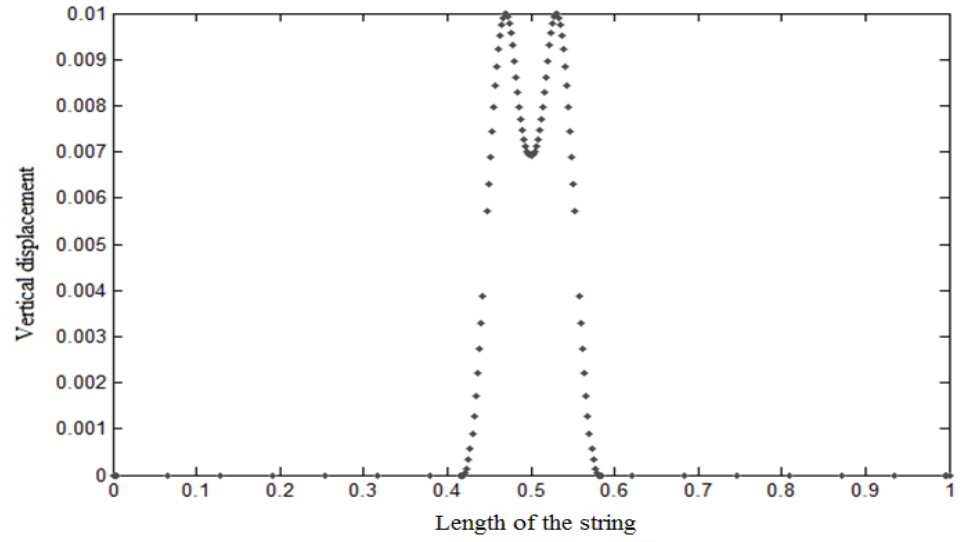

(a)

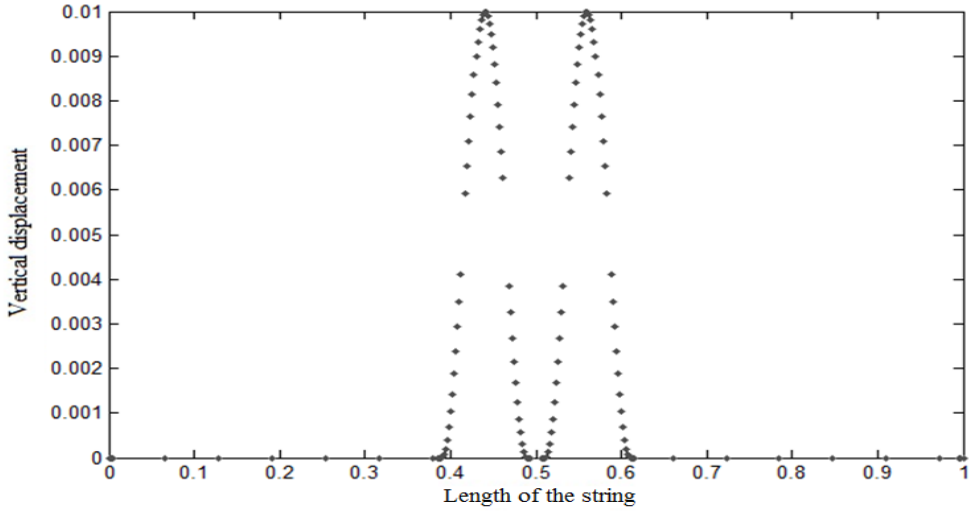

(b)

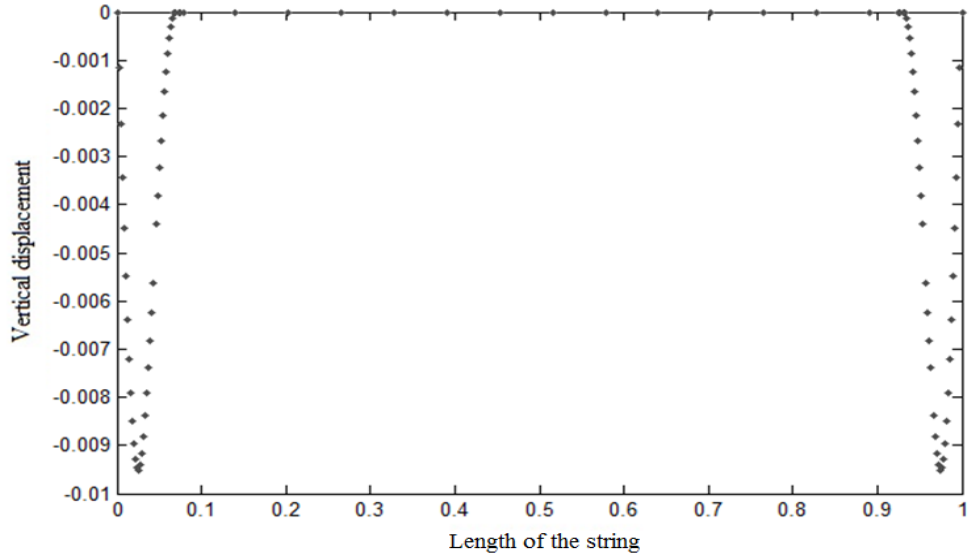

(c)

Fig. 13. Vertical displacement of the string at various time steps; (a) $t = 0.03$, (b) $t = 0.06$, (c) $t = 0.52$. In this problem, time and length variables are dimensionless

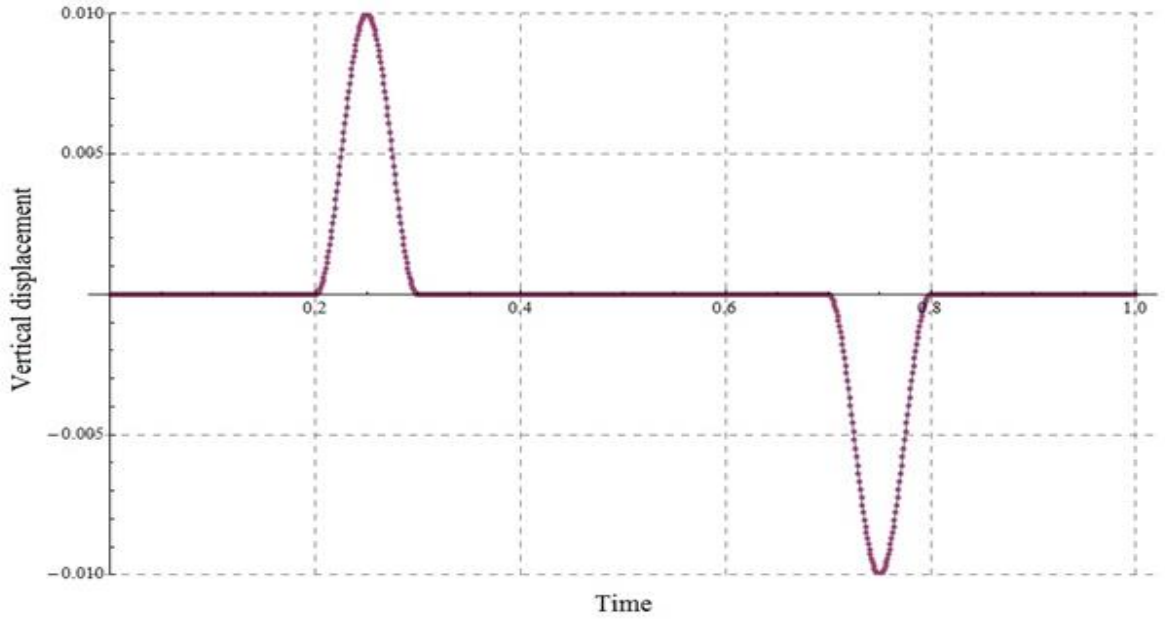

Fig. 14. The second example; Vertical displacement of the string ($x = 0.25$)

Free Vibration of an Infinite Beam

In the last example, flexural wave propagation in the Euler-Bernoulli beam was examined. Consider an infinite beam with the following initial excitations:

$$y(x,0) = e^{-x^2/64}, \quad \dot{y}(x,0) = 0 \qquad (23)$$

in which *y* represents transverse deflection, and *x* denotes the longitudinal axis of the beam. In addition, the dot superscript indicates the derivative of the transverse deflection with respect to time (that is, initial velocity of the beam). For this type of initial and boundary conditions, the analytical solution is available by using integral transform (Fourier, 1822). It is clear that the velocity of flexural wave in the Euler-Bernoulli beam strongly depends on the frequency content of the wave. This phenomenon may be related to shortcomings of this theory compared to higher order theories, such as the Timoshenko beam theory (1974). For the case of infinite members of this example, when the propagating wave reaches the end cells, required cells would be added to the solution domain. Furthermore, the required points for the D-D scheme were added to the solution domain from both sides of the domain, when needed. The selected loading includes the entire range of existing frequencies, whose participation is different. As pointed out earlier, these frequencies would be separated due to time marching process. When the participation of a specific frequency is smaller than the D-D threshold, this frequency would be eliminated. Figure 15 shows the transverse displacement of the specified points obtained from the analytical and study's methods.

Furthermore, Figure 16 represents the snapshot solutions corresponding to two various moments ($e = 5\mathrm{E}-6$). As shown in Figure 16, dense solution points are present in the wave-front. This phenomenon is related to high frequency waves traveling with higher wave velocities. As a result, we may conclude that for the case of loading, the Euler-Bernoulli based models may not provide acceptable results.

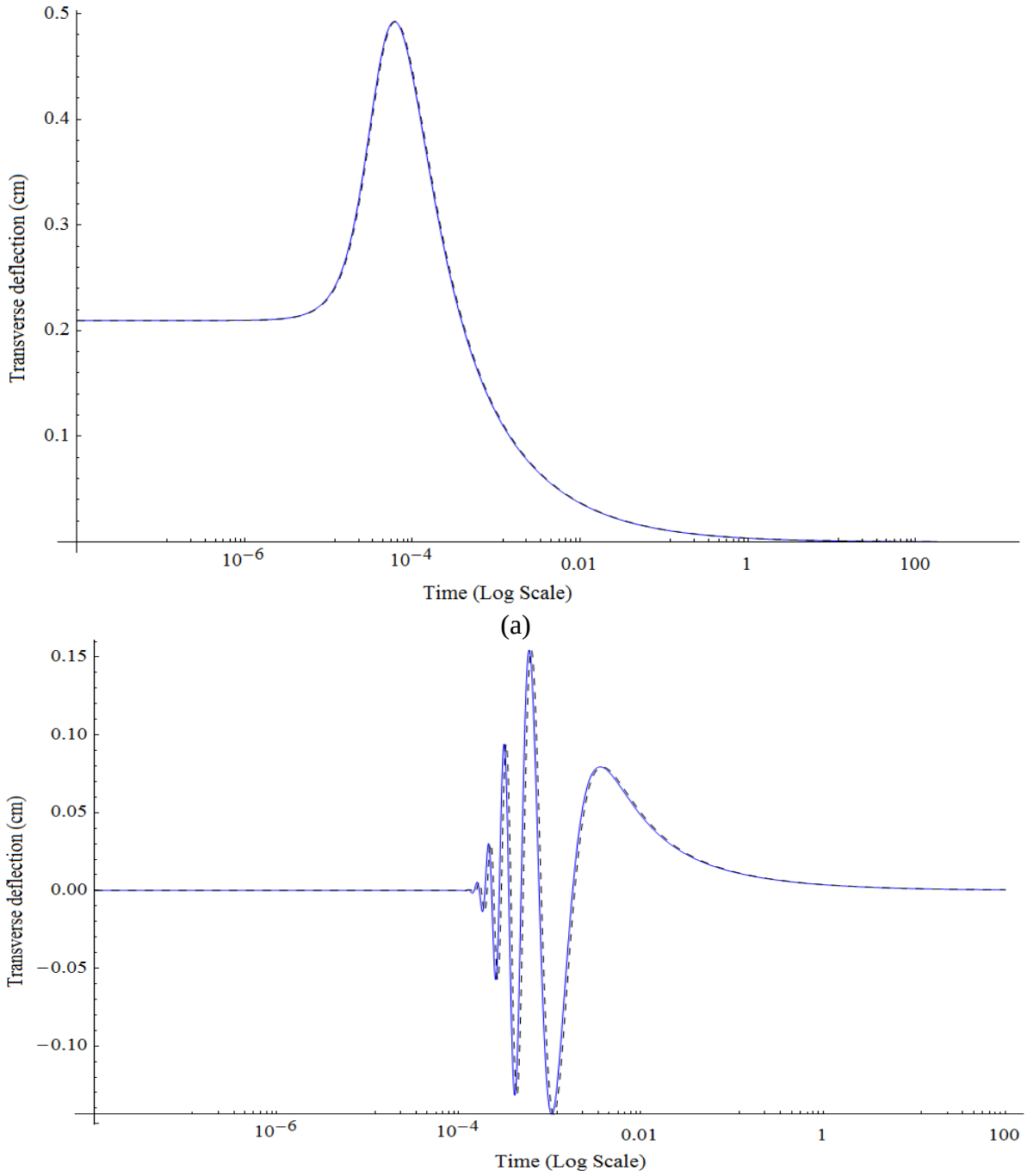

Fig. 15. Transverse displacement of the beam at (a) $x = 10$ cm, and (b) $x = 100$ cm; The study's method and analytical method are represented with dashed-black and solid-blue lines, respectively.

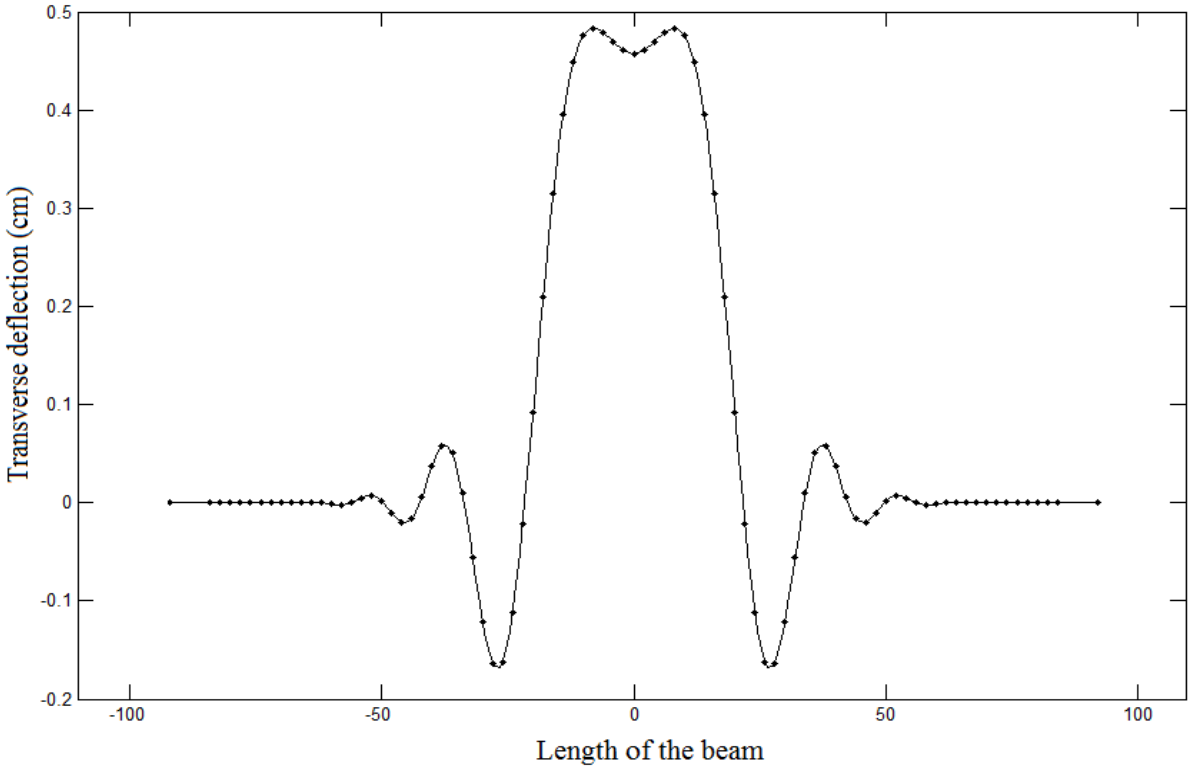

(a)

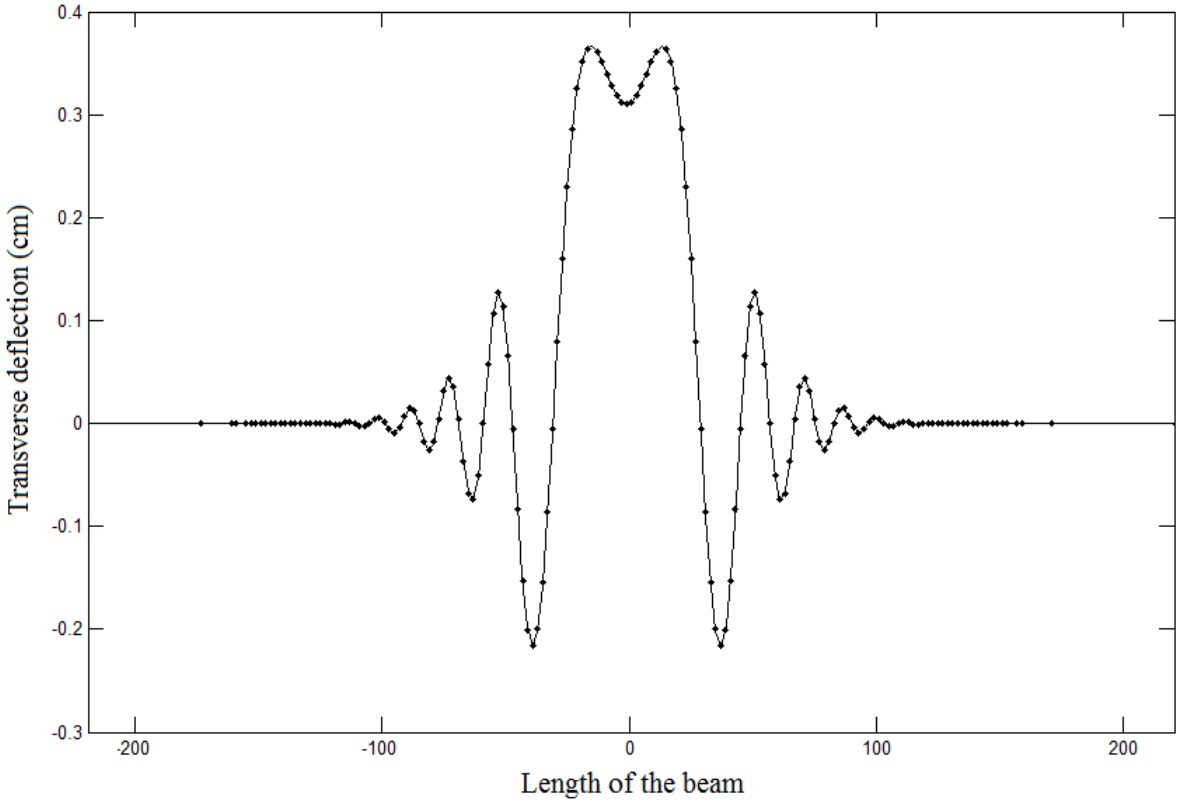

(b)

Fig. 16. Transverse deflection of the Euler-Bernoulli beam at (a) $t = 0.08$ ms, and (b) $t = 0.16$ ms

CONCLUSIONS

In this research, an adaptive method was developed for solving wave motion problems of one-dimensional domains. At first, considering the conservation of mass and the balance of momentum, a physics-based method was developed. Afterwards, adaptive points of discretized domain were determined using the D-D wavelets. The advantages of the CA method as an efficient method for the solution of these types of problems are promising. The results of the present method are in excellent agreement with those reported in literature and those achieved by analytical solutions. When compared to other existing numerical methods, the present method directly obtains all unknowns of the problem which have physical meanings (e.g., stresses, strains, internal forces); whereas other well-known numerical methods, need to calculate derivatives or other post-processing operations to get these unknowns.

REFERENCES

Chopard, B. (1990). "A cellular automata model of large-scale moving objects", *Journal of Physics A*, 23(10), 1671-1687.

Chopard, B. and Droz, M. (1988). "Cellular automata approach to non-equilibrium phase transitions in surface reaction model: static and dynamic properties", *Journal of Physics A*, 21(1), 205-211.

Chopard, B., Droz, M. and Kolb, M. (1989). "Cellular automata a roach to non-equilibrium diffusion and gradient percolation", *Journal of Physics A*, 22, 1609-1619.

Chopard, B., Luthi, P.O. and Queloz, P.A. (1996). "Cellular automata model for car traffic in two-dimensional street networks", *Journal of Physics A*, 29, 2325-2336.

Courant, R., Friedrichs, K. and Lewy, H. (1928). "About the partial differential equations of mathematical physics (in German)", *Mathematische Annalen*, 100, 32-74.

Cruz, P., Mendes, A. and Magalhães, F.D. (2001). "Using wavelets for solving PDEs: an adaptive collocation method", *Chemical Engineering Science*, 56(10), 3305-3309.

Deslauriers, G. and Dubuc, S. (1989). "Symmetric iterative interpolation processes", *Constructive Approximation*, 5, 49-68.

Donoho, D.L. (1992). *Interpolating wavelet transforms tech*, Report 408, Department of Statistics, Stanford University, Stanford, CA, U.S.A.

Fourier, J.B. (1822). *The analytical theory of heat*, Chez Firmin Didot, pere et fils, Paris, France, (in French).

Frisch, U., d'Humieres, D., Hasslacher, B., Lallemand, P., Pomeau, Y. and Rivet, J.P. (1987). "Lattice gas hydrodynamics in two and three dimensions", *Complex Systems*, 1(4), 649-707.

Jameson, L.M. (1998). "A wavelet-optimized, very high order adaptive grid and order numerical method", *SIAM Journal of Scientific Computing*, 19(6), 1980-2013.

Holmström, M. (1999). "Solving hyperbolic PDEs using interpolating wavelets", *SIAM Journal of Scientific Computing*, 21(2), 405-420.

Hopman, R.K. and Leamy, M.J. (2011). "Triangular cellular automata for computing two-dimensional elastodynamic response on arbitrary domains", *Journal of Applied Mechanics*, 78(2), 1115-1132.

Kawamura, S., Shirashige, M. and Iwatsubo, T. (2005). "Simulation of the nonlinear vibration of a string using the cellular automation method", *Journal of Applied Acoustics*, 66(1), 77-87.

Kawamura, S., Yoshida, T., Minamoto, H. and Hossain, Z. (2006). "Simulation of the nonlinear vibration of a string using the cellular automata based on the reflection rule", *Journal of Applied Acoustics*, 67(2), 93-105.

Kwon, Y.W. and Hosoglu, S. (2008). "Application of lattice Boltzmann method, finite element method, and cellular automata and their coupling to wave propagation problems", *Computers and Structures*, 86(7), 663-670.

Leamy, M.J. (2008). "Application of cellular automata modeling to seismic elastodynamics", *International Journal of Solids and Structures*, 45(17), 4835-4849.

Liu, Y., Cameron, I.T. and Wang, F.Y. (2000). "The wavelet collocation method for transient problems with steep gradients", *Chemical Engineering Science*, 55(9), 1729-1734.

Mallat, S. (1999). *A wavelet tour of signal processing*, Academic Press, New York, U.S.A.

Reinsch, C.H. (1971). "Smoothing by spline functions II", *Numerische Mathematik*, 16(5), 451–454.

Rothman, D.H. (1987). "Modeling seismic P-waves with cellular automata", *Geophysical Research Letters*, 14(1), 17-20.

Schreckenburg, M., Schadschneider, A., Nagel, K. and Ito, N. (1995). "Discrete stochastic models for traffic flow", *Physical Review E*, 51(4), 2939-2949.

Timoshenko, S. (1953). *History of strength of materials*, McGraw-Hill, New York, U.S.A.

Timoshenko, S., Young, D.H. and Weaver, W. (1974). *Vibration problems in engineering*, Wiley, New York, U.S.A.

Vasilyev, O.V. and Paolucci, S. (1996). "A dynamically adaptive multilevel wavelet collocation method for solving partial differential equations in a finite domain", *Journal of Computational Physics*, 125(2), 498-512.

von Neumann, J. (1966). *Theory of self-reproducing automata*, University of Illinois Press, Urbana, IL, U.S.A.

Wolfram, S. (2002). *A new kind of science*, Wolfram media, U.S.A.

Yang, K. (2008). "A unified solution for longitudinal wave propagation in an elastic rod", *Journal of Sound and Vibration*, 314(1), 307-329.